NAWCWPNS TP 8124

Enhanced Down-Range Profiles of Complex Targets Using Wideband Radar Echo Returns

by
Brett Borden
Physics Division
Research Department

MAY 1993

NAVAL AIR WARFARE CENTER WEAPONS DIVISION
CHINA LAKE, CA 93555-6001

Naval Air Warfare Center Weapons Division

FOREWORD

The research described in this report was performed during the 1993 fiscal year as part of an effort to improve radar classification and identification capabilities for non-cooperative targets. This problem continues to be a primary goal of radar research programs and considerable effort has been expended within the last few decades in attempts to solve it. The accuracy of these methods depends upon available radar resolution and so, indirectly, it depends on radar bandwidth.

A novel technique for radar-based non-cooperative target recognition (NCTR) has been created and verified using a variety of real and synthesized data. This method uses ordinary azimuth-elevation phase monopulse measurements and is appropriate for application in existing (narrow-band) missile systems. An enhancement has also been developed (using wide-band measurements) and offers significantly greater target classification ability. This synopsis briefly describes this practical algorithm and lists its required input data as well as displaying an example of its merit.

This effort was supported by ONR Code 1264.

This report was reviewed for technical accuracy by Carey Schwartz.

Approved by
R. L. DERR, *Head*
Research Department
24 May 1993

Under authority of
W. E. NEWMAN
RAdm., U.S. Navy
Commander

Released for publication by
S. HAALAND
Deputy Commander for Research and Development

NAWCWPNS Technical Publication 8124

Published by . . . . . Technical Information Department
Collation . . . . . Cover, 7 leaves
First printing . . . . . 65 copies

REPORT DOCUMENTATION PAGE

Form Approved
OMB No 0704-0188

1 AGENCY USE ONLY *(Leave blank)*	2 REPORT DATE	3 REPORT TYPE AND DATES COVERED
	May 1993	Interim Oct—Dec 1992

4 TITLE AND SUBTITLE
ENHANCED DOWN-RANGE PROFILES OF COMPLEX TARGETS USING WIDEBAND RADAR ECHO RETURNS

5 FUNDING NUMBERS
WU 113132
PE 61153N
TA BR052-02-01

6 AUTHOR(S)
Brett Borden

7 PERFORMING ORGANIZATION NAME(S) AND ADDRESS(ES)
Naval Air Warfare Center Weapons Division
China Lake, CA 93555-6001

8 PERFORMING ORGANIZATION REPORT NUMBER
NAWCWPNS TP 8124

9 SPONSORING/MONITORING AGENCY NAME(S) AND ADDRESS(ES)
Office of Naval Research
Arlington, VA 22217-5000

10 SPONSORING/MONITORING AGENCY REPORT NUMBER

11 SUPPLEMENTARY NOTES

12A DISTRIBUTION/AVAILABILITY STATEMENT
A Statement, public release, distribution unlimited

12B DISTRIBUTION CODE

13 ABSTRACT *(Maximum 200 words)*

(U) Small radar detection and tracking systems—in particular, radar guided missile systems—are of great utility because of their all-weather performance and their long range capabilities A major drawback with these systems results from the relatively simple data that they collect and the difficulty in using these data for target classification and identification purposes We propose a technique which employs the statistics of the tracking data used by many missile seekers and which creates a cross-range target structure map that can be expressed as a function of the target's down-range extent These data consist of ordinary azimuth-elevation phase monopulse measurements collected from a small set of (unknown) aspects presented by the target as it maneuvers The method requires a minimal computational burden and holds the potential to be used for automatic (machine-based) target classification in realistic (time and data limited) environments

14 SUBJECT TERMS	15 NUMBER OF PAGES
Glint, Identification, Radar, Target ID	13
	16 PRICE CODE

17 SECURITY CLASSIFICATION OF REPORT	18 SECURITY CLASSIFICATION OF THIS PAGE	19 SECURITY CLASSIFICATION OF ABSTRACT	20 LIMITATION OF ABSTRACT
UNCLASSIFIED	UNCLASSIFIED	UNCLASSIFIED	UL

INTRODUCTION

A problem of recurring interest to radar engineers concerns the classification and identification of aircraft which do not broadcast their own identity. So-called *non-cooperative target recognition* (NCTR) continues to be a primary goal of radar research programs and considerable effort has been expended within the last few decades in attempts to solve it. Unfortunately, to date, few "appropriate" techniques (and even fewer "practicable" techniques) have been developed.

The variety of radar-based methods that have been suggested for NCTR can be divided into two general groups: those which make use of some physical process unique to the target and those which attempt to "image" the target itself. The physical process group includes methods based upon engine modulations (JEM), nonlinear-contact effects (metal-metal junctions on the target), as well as proposed methods based on skin vibrational modulation effects. The imaging category encompasses SAR/ISAR based methods, down-range profiling, high-resolution angle imaging, and a variety of techniques collectively known as "inverse scattering reconstruction" and which actually attempt to create only a generalized "image" of the target. (Cf., [References 1 through 3], and references cited therein.)

The limited success of these approaches often results from a failure to properly account for restrictions imposed by realistic radar/target environments. JEM, for example, can be considered to be the most successful of all the methods but may only be used when the target orientation allows the engine turbine blades to be "seen" by the radar. Other "physical-process" based techniques have never been convincingly applied to NCTR. The shortcomings in this first category of methods have motivated most researchers to concentrate their efforts on perfecting imaging approaches. Microwave imaging attempts, with radar, to do what is usually accomplished with conventional light sources. However, since image resolution is proportional to the aperture-to-wavelength ratio, potential systems require too-large apertures for many applications of interest. (Reduction of wavelength cannot be done indiscriminately since atmospheric attenuation and adverse weather conditions severely limit the usable range of the imaging system—this precludes optical imaging systems from potential long-range NCTR schemes.) The aperture can be synthetically increased, of course, but synthetic aperture imaging requires accurate determination of target aspect over time (an often lengthy and unreliable task). Full-blown inverse scattering methods suffer even more from restrictions on the necessary data: they not only require that the data be matched to known target aspect angles but they also frequently require that these data be collected over large bandwidths.

Finally, down-range target profiling has been suggested as a classification alternative. (This has been much ballyhooed in connection with ultra-wideband radar research.) In its simplest form, a down-range profile consists of target scatterer strength integrated over a sequence of range-bins and mapped to the target's down-range extent. When target orientation is known in advance, this can yield crude target structure information and may be used for rudimentary target classification. However, the target's orientation is usually

not known in advance (it is usually estimated from a detailed target track) and a preferable scheme would yield target orientation as part of the image In addition, the simple down-range profile cannot really offer the amount of information required for meaningful target classification

In addition to long-range and all-weather requirements (which can be satisfied only by radar systems), the chosen recognition/classification scheme must be tailored to the platform on which it will be used This consideration usually restricts the type of data that can be employed and the computational engine that will process these data One of the most restrictive environments are that of the small, radar-based missile system—and it is this problem that we shall address below Typically, radar missile seekers devote most of their resources to the problems of guidance and control and have little (if any) ability to acquire data which are not related to these primary responsibilities

Our present discussion demonstrates how ordinary phase monopulse tracking data can be used to create an enhanced down-range target profile that offers considerably greater information than usual profiles Phase monopulse data consist of measurements of the gradient of the phase-front of the field scattered from the target. Tacking information is deduced from this gradient since, for a point scatterer, both gradient and target bearing lie normal to the spherical phase-front [Reference 4]. However, extended targets will not generally scatter spherically symmetric wave fronts and the phase gradient can only be expected to point to the target on average. We begin by examining the statistical behavior of this kind of data and show how these statistics are related to the target's cross-range structure Then we extend these results to large bandwidth signals. (Wideband signals have been proposed for use in missile systems in an effort to mitigate the so-called "glint" problem, which we shall discuss in the conclusion.) Finally, we present some examples using computer generated data that demonstrate the algorithm's behavior under ideal conditions.

PHASE DERIVATIVE STATISTICS

The original application of phase gradient statistics to target structure estimation was performed for narrowband signals in [References 5 and 6]. We briefly review the narrowband results here for completeness and because they form the basis for the related wideband results.

We fix a coordinate system to the target and consider a monostatic scattering situation in which the transmitter and receiver are co-located. In the weak scatterer approximation the (scaled) far-field response $F_S(\mathbf{x},t)$, at position $\mathbf{x}$ and time t, to a signal $F_I(\mathbf{y},t)$ incident upon the target is simply the sum of the responses from individual elements of the target. The scattered field can be written as

$$F_S(\mathbf{x},t) = \int_D F_I(2\mathbf{y}, t - 2|\mathbf{x}|/c)\, \rho(\mathbf{y})\, d\mathbf{y} \,, \tag{1}$$

where D is the support of the local scatterer density function $\rho(\mathbf{y})$, c is the signal speed, and the factor of 2 accounts for the (two-way) signal travel distance

In the quadrature model F_S is analytic, with real and imaginary parts forming a Hilbert transform pair, and we can write $F_S(\mathbf{x},t) = |F_S(\mathbf{x},t)| exp(i\varphi(\mathbf{x},t))$ where $\varphi(\mathbf{x},t)$ is the phase of the scattered field. Let $\hat{\mathbf{n}}$ denote the direction of signal propagation If $\hat{\mathbf{u}}$ is a unit vector perpendicular to $\hat{\mathbf{n}}$ then the directional, derivative of this phase can be found from

$$\hat{\mathbf{u}} \cdot \nabla\varphi(\mathbf{x},t) = Im\left(\frac{F_S^*(\mathbf{x},t)}{|F_S(\mathbf{x},t)|^2} \hat{\mathbf{u}} \cdot \nabla F_S(\mathbf{x},t) \right). \tag{2}$$

$F_I(\mathbf{y},t)$ must satisfy the wave equation and can be written $F_I(\mathbf{y},t) = F_I(\hat{\mathbf{n}} \cdot \mathbf{y} - ct)$. Substitution yields

$$\hat{\mathbf{u}} \cdot \nabla\varphi(\mathbf{x},t) = Im\left(\frac{F_S^*(\mathbf{x},t)}{|F_S(\mathbf{x},t)|^2} \int_D \frac{2\hat{\mathbf{u}} \cdot \mathbf{y}}{|\mathbf{x}|} \rho(\mathbf{y}) F_I'(2|\mathbf{x}| + 2\hat{\mathbf{n}} \cdot \mathbf{y} - ct) d\mathbf{y} \right) \tag{3}$$

where $F_I'(\xi) = dF_I(\xi)/d\xi$

Since the coordinate system is fixed to the target, a measured value $g_i = g(\hat{\mathbf{n}}_i) = \hat{\mathbf{u}} \cdot \nabla\varphi(\mathbf{x}_i,t)$ will depend upon the target orientation through the "weighting" function $\rho(\mathbf{y})$. Moreover, in typical radar situations the signal has high frequency content (~10 GHz) and g_i varies rapidly with only minute changes in target aspect. (It is known, for example that measurements from targets flying "straight and level" will exhibit significant variation.) For this reason, we consider $\rho(\mathbf{y})$ to be a random process and examine the statistical behavior of g_i.

The narrowband case When we set $F_I(\mathbf{y},t) = exp\left(\imath k(\hat{\mathbf{n}}\ \mathbf{y} - ct)\right)$ where $k = \omega / c$ is the wave number associated with the time harmonic incident field of frequency ω, we obtain

$$\hat{\mathbf{u}}\ \nabla\varphi(\mathbf{x},t) = Im\left(\imath \frac{F_S^*(\mathbf{x},t) e^{\imath(2k|\mathbf{x}| - \omega t)}}{|F_S(\mathbf{x},t)|^2} \int_D \frac{2k\hat{\mathbf{u}}\ \mathbf{y}}{|\mathbf{x}|} \rho(\mathbf{y}) exp(\imath 2k\hat{\mathbf{n}}\ \mathbf{y}) d\mathbf{y} \right) \tag{4}$$

Define $G(\mathbf{x},t) = |G(\mathbf{x},t)| e^{\imath\psi(\mathbf{x},t)} \equiv \hat{\mathbf{u}}\ \nabla F_S(\mathbf{x},t)$ Then Equation (4) becomes

$$\hat{\mathbf{u}}\ \nabla\varphi(\mathbf{x},t) = \frac{|G(\mathbf{x},t)| cos(\psi(\mathbf{x},t) - \varphi(\mathbf{x},t))}{|F_S(\mathbf{x},t)|} \tag{5}$$

We model the target as a collection of N point scatterers and write $\rho(\mathbf{y}) = \sum_{n=1}^{N} A_n e^{\imath\vartheta_n} \delta(\mathbf{y} - \mathbf{y}_n)$. Each of the independent random variables $\{A_n\}$ and $\{\vartheta_n\}$ are assumed to be uncorrelated and strict-sense stationary for all n =1,.. ,N In addition, we assume that $\{\vartheta_n\}$ is uniform in the interval $(-\pi, \pi)$. This model yields

$$|F_S| = \left|\sum_n S_n\right| \qquad \text{where} \quad S_n \equiv A_n exp\left[\imath(2k\hat{\mathbf{n}} \cdot \mathbf{y}_n + \vartheta_n)\right] \tag{6}$$

(and similarly for $|G|$) It is easy to show that, for large N, the quantity $\sum_n S_n$ is a normally distributed mean zero random variable (this follows from the Central Limit Theorem [Reference 7]). It follows that $|F_S(\mathbf{x},t)|$ and $|G(\mathbf{x},t)|$ are independent Rayleigh distributed random variables

The $\varphi(\mathbf{x},t)$ and $\psi(\mathbf{x},t)$ are independent and so the numerator in Equation (5) is a normally distributed random variable The probability density of $g(\hat{\mathbf{n}}) = \hat{\mathbf{u}} \cdot \nabla\varphi(\mathbf{x},t)$ follows as the density of the quotient of independent normal and Rayleigh random variables We obtain

$$f_s(g,\hat{\mathbf{u}}) = \frac{\kappa^2}{2\left(\kappa^2 + g^2\right)^{3/2}} \tag{7}$$

where

$$\kappa^2(\hat{\mathbf{u}}) \equiv \frac{E\{GG^*\}}{E\{F_S F_S^*\}} = \frac{1}{N}\sum_{n=1}^{N}\left(\frac{2k\hat{\mathbf{u}}\ \mathbf{y}_n}{|\mathbf{x}|}\right)^2 \tag{8}$$

The target shape information available from the measured $\{g_i\}$ comes through κ^2 which depends upon the support D of $\rho(\mathbf{y})$ and can be deduced by comparing the statistics of $\{g_i\}$ to Equation (7) (see below).

The simple form of Equations (7) and (8) is a direct consequence of our target model—in particular, on the assumption that ϑ_n is uniform on $(-\pi,\pi)$. However, the qualitative behavior of these results is unaltered by more general assumptions [Reference 8]. We have opted for this simpler approach because it is significantly more tractable and because, at high frequencies ($\omega \approx 10$ GHz), the net error is equivalent to a tiny down-range shift in $\rho(\mathbf{y})$. The assumptions on D are more important since if the support of $\rho(\mathbf{y})$ is too restricted then the sums implied by the integrals (6) will not satisfy the requirements of the central limit theorem. For this reason, we consider only "complex" targets (by which we mean targets with sufficient scattering centers that Equations (8) and (9) are good approximations)

One additional assumption is required. In practice, the direction $\hat{\mathbf{u}}$ is fixed to the receiver and so the statistics of $\{g_i\}$ will depend on target orientation. This dependence is not nearly so sensitive as the dependence of the individual measurements g_i on target aspect (which we have already discussed) However, we must assume that the target is changing its aspect at a sufficiently slow rate that the data set $\{g_i\}$ can be considered to have been collected over a small domain (say < 10°) of target orientations. (In practice, we have obtained good results with data sets of only a few dozen samples and so, this is not really much of a restriction.)

The derivative of the scattered field phase with respect to wave number is given by

$$\left.\frac{d\varphi(\mathbf{x},t)}{dk}\right|_{t=2|\mathbf{x}|/c} = Im\left(\iota\,\frac{F_S^*(\mathbf{x},t)e^{\iota(2k|\mathbf{x}|-\omega t)}}{\left|F_S(\mathbf{x},t)\right|^2}\int_D 2\hat{\mathbf{n}}\ \mathbf{y}\rho(\mathbf{y})exp(\iota 2k\hat{\mathbf{n}}\ \mathbf{y})d\mathbf{y}\right). \tag{9}$$

Comparing (9) with Equation (4), we can see that the statistics of this measurement are fundamentally the same as for the cross-range derivatives except that the parameter $\kappa^2(\hat{\mathbf{n}})$ will be determined by the down-range properties of the target It is easy to see, by substituting $\hat{\mathbf{u}} = \hat{\mathbf{i}}\cos\theta + \hat{\mathbf{j}}\sin\theta$ into Equation (8) that $\kappa(\theta) = \sqrt{\kappa^2(\theta)}$ defines an ellipse whose shape and orientation depend upon the cross-range extent of the target The combination $\left(\kappa^2(\hat{\mathbf{u}}), \kappa^2(\hat{\mathbf{n}})\right)$ will define an ellipsoid whose shape and orientation are determined by the target as a whole. This ellipsoid can be mapped to overall target dimensions and orientation. However, it seems doubtful that this information can ever be used for more than rough target categorization. A more promising approach uses a modified estimate $\kappa^2(\hat{\mathbf{u}};t)$ determined as a function of the target's down-range extent

The wideband case The narrowband result is sufficiently interesting that we want to preserve as much of its character as possible. To do this, we select the incident signal to be of the form $F_I(\mathbf{y},t) = E(\hat{\mathbf{n}}\ \mathbf{y} - ct)exp\left(\iota k_o(\hat{\mathbf{n}}\ \mathbf{y} - ct)\right)$ where k_o is the wave number associated with a "carrier" frequency ω_o and $E(ct) = |E(ct)|e^{\iota\varepsilon(ct)}$ is an "envelope" function with compact support.

Let $\xi \equiv 2|\mathbf{x}| + 2\hat{\mathbf{n}}\ \mathbf{y} - ct$. We require $E(\xi)$ to be slowly varying in comparison with the carrier frequency:

$$\left|\frac{E'(\xi)}{E(\xi)}\right| << k_o \tag{10}$$

Then the remaining derivation follows as before and we can conclude that $f_g(g;\hat{\mathbf{u}})$ obeys Equation (7) with

$$\kappa^2(\hat{\mathbf{u}},t)=\frac{1}{\sum_{n=1}^{N}\left|E(\xi_n)\right|^2}\sum_{n=1}^{N}\left(\frac{2k\,\hat{\mathbf{u}}\cdot\mathbf{y}_n}{|\mathbf{x}|}\right)^2\left|E(\xi_n)\right|^2 \tag{11}$$

The presence of $|E(\xi)|^2$ in (11) reduces the support of the summations to the intersection of the support of $|E(\xi)|$ and D. As ξ varies with t, D will be effectively "sliced" into a collection of down-range components. The statistics of (7) and (11) allow us to associate a relevant cross-range target structure measure to each down-range slice.

ESTIMATION OF κ^2

For a direction $\hat{\mathbf{u}}$ fixed to the receiver, we can collect a set of phase-front derivative data $\{g_i\}$, $i = 1,\ldots,P$, associated with P (unknown) target aspect angles. Assuming that these aspects angles have sufficiently small variation that the statistics of Equation (7) are quasi-stationary, then we can use statistical estimation techniques to determine $\kappa^2(\hat{\mathbf{u}})$.

The maximum likelihood estimator for $\kappa^2(\hat{\mathbf{u}})$ will be the one that maximizes the function

$$\Lambda(\kappa^2)=\prod_{i=1}^{P}\frac{\kappa^2/2}{\left(\kappa^2+g_i^2\right)^{3/2}}\,. \tag{12}$$

(Here, we choose to maximize the log-likelihood for convenience.) Differentiating $\ln\Lambda(\kappa^2)$ with respect to κ^2 and setting the result to zero yields

$$\frac{P}{3}-\sum_{i=1}^{P}\frac{\kappa^2/2}{\kappa^2+g_i^2}=0\,. \tag{13}$$

Equation (13) is the sum of functions of the form

$$\frac{1}{3} - \frac{\kappa^2/2}{\kappa^2 + g_i^2} \tag{14}$$

and so it will possess only two real solutions which are located symmetrically about the origin. The magnitude of either zero is our desired estimate and can be obtained numerically from Equation (13).

THE DOWN-RANGE MAP ASSOCIATED WITH A TARGET

As $\hat{\mathbf{u}}$ is allowed to vary, we will obtain a collection of estimates for $\kappa^2(\hat{\mathbf{u}})$—each a solution to Equation (13) using the associated input data $\{g_i = \hat{\mathbf{u}} \cdot \nabla\varphi(\mathbf{x}_i, t_j)\}$. In a standard Cartesian coordinate system, with axes directions $\hat{\mathbf{i}}$ and $\hat{\mathbf{j}}$, we can associate a polar coordinate angle by $\hat{\mathbf{u}} \cdot \hat{\mathbf{i}} = \cos(\theta)$. The values of $\kappa(\theta)$ will, ideally, trace out an ellipse of the form

$$\kappa(\theta) = \frac{d}{1 + e\cos[2(\theta + \alpha)]} . \tag{15}$$

We can use least-squares estimation to fit a set of estimates $\{\kappa_k^2 \equiv \kappa^2(\theta_k)\}, k = 1,...,K$ to the ideal form of Equation (15). This will allow us to associate the parameter set $\{d, e, a\}$ to each data set $\{\nabla\varphi(\mathbf{x}_i, t)\}$. These parameters are related to target cross-range extent (through d), cross-range shape (through e), and target orientation (through a). Moreover, if the data are of large enough bandwidth that we can isolate separate slices of down-range components as in Equation (11), then we can associate these structure and orientation parameters to a down-range map of the target.

AN EXAMPLE

For verification purposes, we model a synthetic target as a collection of point scatterers with fixed amplitudes, phases, and locations, and calculate the appropriate azimuth and elevation data that would be obtained by a phase-monopulse tracking system trained on the randomly maneuvering target. We have created these data with sufficient bandwidth that we can associate $i = 1, ...,P$ data values $\{\nabla\varphi(\mathbf{x}_i, t_j)\}$ to each of $j = 1,...,M$ down-range target slices. These data are vector-valued with components consisting of the

azimuth and elevation phase derivatives. The interval $(0,\pi)$ was subdivided into $k = 1,\ldots,K$ equal subintervals and the directions $\hat{\mathbf{u}}_k = \hat{\mathbf{i}}\cos\theta_k + \hat{\mathbf{j}}\sin\theta_k$ were used to create the values $g_i(t_j) = \hat{\mathbf{u}}_k \nabla\varphi(\mathbf{x}_i, t_j)$ which were input into Equation (13) to estimate $\kappa^2(\hat{\mathbf{u}}_k, t_j)$. Finally, these values were fit to the ellipses of Equation (15) to determine the target parameters $\{d(t_j), e(t_j), \alpha(t_j)\}$.

Figure 1 displays a collection of 200 point scatterers randomly placed on the skin of a synthetic target. From this collection of scatterers we calculated the (wideband) azimuth and elevation phase monopulse tracking data for each of 100 random target orientations chosen from within a $10° \times 10°$ domain centered on the target's axis. We have modeled the incident signal as positively directed along the z-axis with carrier frequency 30 GHz and simple unit-box envelope characterized by a bandwidth of 1 2 GHz. Figure 2 shows the results of the algorithm displayed in graphical format This image is the "enhanced down-range map" and clearly shows the influence of target cross-range structure in an interpretable way.

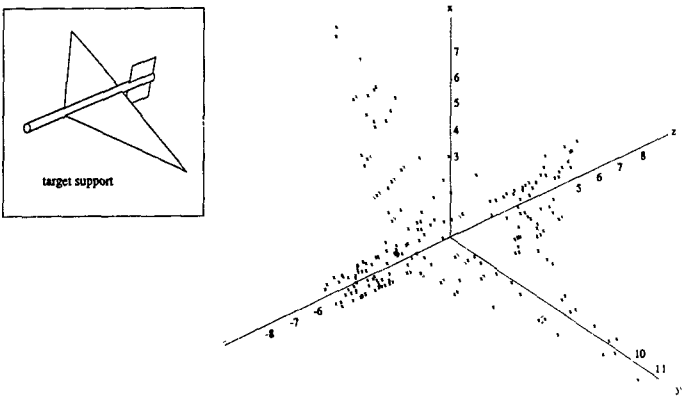

FIGURE 1. Sample Target Plotted are the location of the 200 scattering centers in space These scattering centers were chosen to be randomly located on the surface of the target and obey the approximate relation of 10 scatterers per down-range slice (Target support and orientation are shown in the inset) Not plotted are the intensity and phase shift associated with each scatterer.

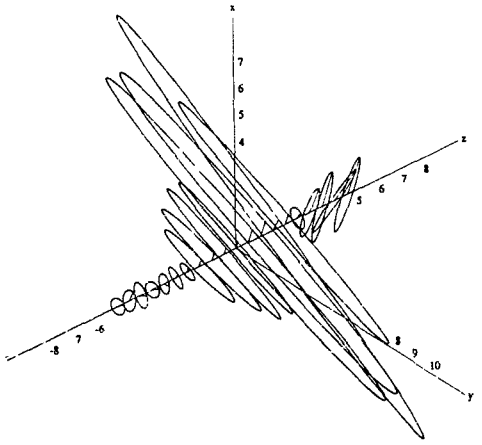

(a) Displays the down-range map as estimated by the algorithm

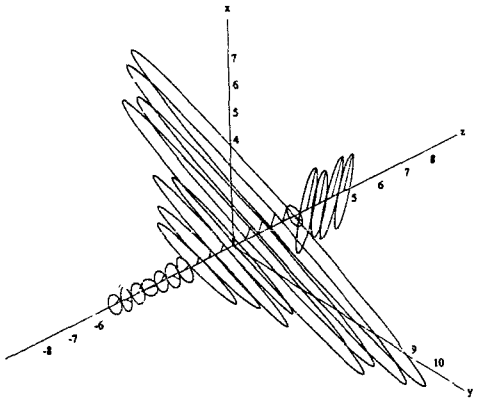

(b) Shows the actual results for this target calculated from Equation (11).

FIGURE 2 Enhanced Down-Range Maps Associated With Target 1.

Note that errors in α diminish the interpretability of the visual reconstruction. An easy enhancement which helps to resolve this ellipse misalignment is to average α overall down-range slices for which the ratio of semi-major to semi-minor axes exceeds

some threshold value. We have not performed this averaging here in order that only the relevant properties of the basic algorithm be displayed. The down-range reconstruction of Figure 2 required 1.2 GHz of bandwidth to achieve the displayed resolution. Less bandwidth results in less resolution—600 MHz of bandwidth, for example, would allow us to plot only half of the ellipses of Figure 2. However, in our studies we have seen that even bandwidths as small as 100 MHz have resulted in meaningful classification of 10 meter (synthetic) targets while standard (simple) down-range profiles have proven to be essentially useless. Even for narrowband systems (vanishing bandwidth) we can still determine target size and orientation.

The example target not is intended to represent the actual distribution of scattering centers for any particular aircraft. Real targets cannot be expected to have a uniform distribution of scatterers lying on the surface of a given cross-sectional slice and while they can be quite complex, they may not be composed of as many as 200 points. (Our models were simple expedients and the total number of scattering centers was chosen by requiring ≈10 scatterers per slice.) However, a particular type of aircraft can be expected to possess a unique distribution of scatterers and by virtue of the squared radius weight they are given in Equation (11), the current algorithm should prove to be a sensitive classifier. Furthermore, the complexity of the aircraft (i.e., the number of scattering centers) will generally increase with increasing carrier frequency ω_0 and the number of scatters per slice can approach the example values under a wide variety of situations. (A detailed examination of the dependence of algorithm accuracy on scatterer number is beyond the scope of the present work. Some initial work along these lines was attempted in Reference 5.)

DISCUSSION AND CONCLUSION

The phase-front of the field scattered from a complex target contains a great deal of information about that target. In the forgoing discussion, we have shown how some of that information can be retrieved by ordinary missile seeker systems. In addition, we have detailed a method that relates cross-range target structure to a set of parameters which can be incorporated into a machine-based target classification system.

The proposed technique has been tested using both real and synthetic data and has proven to be an effective discriminator of overall target size and general shape. In addition, the method has continued to yield useful information about the target even when the data are few in number and the model assumptions are significantly relaxed. Of course, throughout this discussion we have implicitly assumed that the radar is "trained on the target." In practice, however, the so-called "glint problem" may prevent this from being done with complete accuracy.

The glint problem (also known as angular scintillation) refers to the error between the target bearing predicted by the direction of the phase gradient and the true target bearing. This difference is also the data that we are using for our cross-range structure algorithm and cannot be estimated if the true target bearing is unknown. Significant progress has been made in solving this problem and in fact, it is known that tracking error can be effectively eliminated by correctly averaging the separate frequency domain returns

collected by wideband systems [Reference 9] It is precisely these wideband radar systems that we have tailored this algorithm to. (Some progress has also been made in eliminating tracking error from narrowband systems [Reference 10] and the ordinary narrowband version of the algorithm can be expected to be implementable as well.)

Future plans include a more complete verification of the method using a larger variety of measured data In addition, we hope to investigate the classifiability of specific aircraft targets by their phase-front derivatives

REFERENCES

1 M I. Skolnik *Introduction to Radar Systems,* 2nd ed. New York, McGraw-Hill, 1980

2. H. P. Baltes, ed *Inverse Scattering Problems in Optics, Topics in Current Physics* New York, Springer-Verlag, 1980.

3. W-M Boerner *Inverse Methods in Electromagnetic Imaging*, NATO ASI Series, Series C: Math Phys. Sci., 143, Reidel, Dordrecht, Holland, 1985.

4. D. R. Rhodes *Introduction to Monopulse* New York, McGraw-Hill, 1959.

5. B. Borden. "High-Frequency Statistical Classification of Complex Targets Using Severely Aspect-Limited Data," *IEEE Trans on Antennas and Propag.*, Vol. 34(12) (1986), pp. 1455-1459.

6. B Borden. "Phase Monopulse Tracking and its Relationship to Non Cooperative Target Recognition," IMA Volumes in Mathematics and its Applications, *Radar and Sonar, Part 2*, ed. by F A Grunbaum, M. Bernfeld, and R. E Blahut, Vol. 39. New York, Springer-Verlag, 1992.

7. M. Loève *Probability Theory* New York, Van Nostrand, 1963.

8. R. H Delano. "A Theory of Target Glint or Angular Scintillation in Radar Tracking, " *Proc IRE*, Vol. 41 (1953), pp. 1778-1784.

9. J M. Loomis III and E. R. Graf "Frequency-Agility Processing to Reduce Radar Glint Pointing Error, " *IEEE Trans on Aerospace and Electron Sys* , Vol 10 (1974), pp 811-820

10 B. Borden "Diversity Methods in Phase Monopulse Tracking—A New Approach," *IEEE Trans on Aerospace and Electron Sys.*, Vol. 27(6) (1991), pp. 877-880

INITIAL DISTRIBUTION

2 Naval Air Systems Command
    AIR-546TB (1)
    AIR-546TE, D. Glista (1)
4 Chief of Naval Research
    J. Cauffman (1)
    Dr. K. Davis (1)
    Dr. R. Madan (1)
    W. Miceli (1)
1 Commander in Chief, U. S. Pacific Fleet, Pearl Harobr (Code 325)
1 Commander, Third Fleet
1 Commander, Seventh Fleet
2 Naval Air Warfare Center, Aircraft Division, Warminster
    Code 3022, Dr. O. Kessler (1)
    Technical Library (1)
4 Naval Command Control and Ocean Surveillence Center, RDTE Division, San Diego
    R. J. Dinger (1)
    P. Hansen (1)
    C. Ramstadt (1)
    Technical Library (1)
2 Naval Postgraduate School, Monterey, CA
    Dr. M. A. Morgan (1)
    Technical Library (1)
5 Naval Research Laboratory
    Code 7500, Dr. J. R. Davis (1)
    Code 7550
      D. Himes (1)
      L. Wagner (1)
    Dr. A. Jordan (1)
    Technical Library (1)
1 Naval War College, Newport
1 Air Force Intelligence Support Agency, Bolling Air Force Base (AFISA/INT, OUWG Chairman)
2 Defense Technical Information Center, Alexandria
1 A. J. Devaney Associates, Ridgefield, CT (Dr. A. J. Devaney)
1 General Dynamics Corporation, San Diego, CA (Dr. C. P. Tricoles)
1 Center for Naval Analyses, Alexandria, VA (Technical Library)
1 Institute for Defense Analyses, Alexandria, VA (Dr. I. Kay)
2 Massachusetts Institute of Technology, Lincoln Laboratory, Lexington, MA
    Dr. R. M. Barnes (1)
    Dr. G. Morse (1)
1 Michigan State University, East Lansing, MI (Prof. K. M. Chen)
1 Ohio State University, Columbus, OH (Dr. E. Walton)
1 University of Illinois, Chicago, IL (Dr. W. Boerner)

ON CENTER DISTRIBUTION

1 Code C0231, B. Reymore
10 Code C02314, B. Borden
1 Code C2156, W. Katzenstein
1 Code C2158, D. Reade
1 Code C2822, D. Paolino
1 Code C29A4, G. Winkler
1 Code C29B5, M. Mumford
1 Code C291, R. Smith
2 Code C2911
H. Brooks (1)
G. Hewer (1)
4 Code C643 (3 plus Archives Copy)